Scaling vertical drag forces in granular media

EUROPHYSICS LETTERS 1 October 2005

Europhys. Lett., **72** (1), pp. 137–143 (2005)
DOI: 10.1209/epl/i2005-10203-3

Scaling vertical drag forces in granular media

G. Hill, S. Yeung and S. A. Koehler
Department of Physics, Emory University - Atlanta, GA 30322, USA

received 20 June 2005; accepted in final form 29 July 2005
published online 31 August 2005

PACS. 81.05.Rm – Porous materials; granular materials.
PACS. 05.20.Jj – Statistical mechanics of classical fluids.
PACS. 83.10.Pp – Particle dynamics.

Abstract. – The average drag forces on intruders slowly plunging into and withdrawing from shallow beds of monodisperse smooth glass beads and of sifted rough sand scale with the immersion depth and lateral dimensions of the intruder. The withdrawal forces are comparable for both types of media; however, the plunging forces for sand are substantially greater than for smooth glass beads. Furthermore, for glass beads, the rescaled plunging and withdrawal forces have two different power law dependences on the immersion depth, with exponents greater than unity.

Introduction. – The fluid-like behavior of dense, quasi-static, granular media is poorly understood, despite its importance for civil, industrial and pharmaceutical applications as well as numerous efforts on behalf of engineers and physicists. The state of a dense granular system is difficult to define and control, due to the indeterminacy of the individual frictional contact forces between particles for any geometrical configuration involving large coordination numbers. This also complicates the determination of the constitutive relations that allow for development of a mean-field description of granular flow [1]. Nonetheless, experimentalists have been able to perform high-quality, reproducible experiments on the flow of dense granular media, and engineers have developed theories for static granular media to predict the stability of sand piles and the pressures on container walls, such as grain silos. Models for certain types of static configurations and certain types of flows have also been formulated [2–8]. On a more practical level, improved quantitative knowledge of drag forces in flowing granular media should prove useful for a large variety of engineering applications and a better understanding of natural disasters such as avalanches and mud slides.

Studying flow around immersed objects has proven extremely important in the development of modern fluid mechanics, opening up new fields such as boundary layers and turbulence. Likewise, the dynamics of intruders, *e.g.* objects immersed and moving through granular media, also have been crucial for understanding both slow and fast granular flows [9–12]. However, to date no general continuum theory describing these flows exists.

Most studies of dense granular drag of slow intruders have focused on horizontal motion [9, 10, 13, 14], or on intruders in draining hoppers [12]. The experimental results depend on the type of granular medium studied, shearing rates [15], and whether the granular pack is

confined or has a free top surface [16]. For example, Albert *et al.* [10] found that the drag on spheroids slowly moving horizontally through monodisperse glass beads is independent of the velocity as well as bead size, and depends linearly on the immersion depth of the intruder and the intruder's projected area. Chehata *et al.* [12] found that the drag forces of cylinders inserted in narrow chutes depends linearly on the granular pressure (stress), and the projected area. Recently, Stone *et al.* [17] investigated wall effects on the force of plunging discs which approach the container bottom, and found that the excess plunging force, relative to the bulk drag force, exponentially increases with decreasing distance from the container bottom. In other experiments the forces on intruders in jammed granular media were investigated, where the medium has been compactified by gentle tapping to maximize the static friction at the container walls [18].

This letter reports new findings for vertical drag forces on intruders moving in shallow beds of granular media where boundary effects are minimal. Two types of monodisperse granular media, sand and glass beads, where the bead diameter varied over a decade, were investigated. Several different shapes of intruders were used, which varied in size over a decade and in some cases were even smaller than the glass beads they were moving through. Two different power laws are identified and for all experiments the mean drag force scaled with the intruder dimensions.

Experimental details. – The drag on vertically moving intruders was experimentally determined using a simple set-up, involving a motorized translation stage and five-digit balance; both controlled by a PC. Intruders of different shapes and sizes were attached via slender rods (diameter 2 mm) to a vertically moving translation stage mounted over a wide cylindrical glass dish (typical diameter 190 mm, height 100 mm) filled with monodisperse granular media. Table I gives the geometric details of the four types of intruders (cubes, spheres, vertical and horizontal rods), and the two types of granular media (glass beads and sifted sand), and the size of the containing dish. The intruders were continuously and slowly plunged and withdrawn from relatively shallow beds of granular media (about 100 mm deep), and the drag force on the moving intruders was measured as excess weight by a digital balance which supported the granular bed. Provided that the plunging and withdrawing velocities were smaller than 5 mm/s, the forces did not vary with velocity, and instead depended on the immersion depth and the intruder's geometry and orientation and details of the granular medium. For glass beads

TABLE I – *Dimensions of four different intruder geometries as well as two types of granular media and two types of containers, all in* mm. *ℓ denotes the width of the cubes and also the diameter of the spheres and rods. L denotes the axial length of the horizontal rods. Z denotes the cube height.*

Intruder shape	
cube	$\ell \times Z = 6.4 \times 6.4, 25 \times 25, 25 \times 6.4$
sphere	$\ell = 3.2, 6.4, 13, 25$
vertical rod	$\ell = 1.6, 3.3, 1.3$
horizontal rod	$\ell \times L = 0.79 \times 52, 3.2 \times 51, 3.2 \times 102, 6.4 \times 51, 6.4 \times 102, 13 \times 34, 13 \times 51, 13 \times 102$
Granular media	
glass beads	$d = 0.2, 0.5, 0.9, 2, 5$
sand	$d = 0.5$
Dish type	
narrow	width = 85, height = 100
wide	width = 190, height = 100

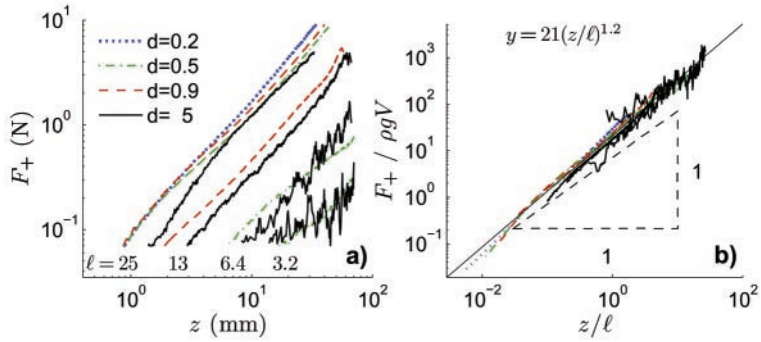

Fig. 1 – a) Average drag forces for plunging spherical intruders, diameter ℓ, into beds of monodisperse glass beads, diameter d, in the wide dish. All reported lengths are in mm. b) Rescaled plunging forces of spheres. The best fit power-curve, shown as a solid line, is included. For comparison, the dashed line shows a linear curve.

no history dependence was observed: successive plunging and withdrawing experiments gave similar force measurements, and for statistical purposes 10 to 50 trials were averaged. This was not the case however for sand, and care was taken to keep track of the shearing history.

Experimental results. – Figure 1a shows how the average plunging forces for spherical intruders, F_+, increases with immersion depth, z, in glass beads (precision glass impact media by Potter Industries Inc.). The plunging force increases with the intruder diameter, ℓ, and is basically independent of the bead diameter, d. When the size of the glass beads is comparable to the spherical intruder ($d \sim \ell$) large fluctuations in the plunging force occur that still remain after averaging over fifty trials. The log-log plot suggests power law behavior for the drag forces. Figure 1b shows that the data indeed collapses nicely upon rescaling the immersion depth z, which is the distance from the top free surface to the *bottom* of the intruder, by the intruder diameter, ℓ, and rescaling the force by $\rho g V$, where ρ is the density of glass ($\rho = 2.46\,\mathrm{g/cm^3}$), g is the gravitational acceleration and V is the sphere volume. Rescaling the withdrawal forces for spherical intruders also collapses the withdrawing data (not shown). In order to test wall effects, the experiments were repeated in a narrower glass dish with the same filling height, and the averaged forces did not change (see tables I and II).

Further plunging and withdrawing experiments were preformed using vertical rods, and cubes, one of which was a truncated cube with height one quarter of the width. The intruder dimensions are given in table I, and the measured forces were close to those for spheres, summarized in table II. The log-log plots and the independence of the drag forces from the intruder's vertical dimension (*i.e.* the truncated cube has similar drag forces as the cube) suggest a power law that only depends on the lateral dimensions:

$$F_\pm / (\rho g A \ell) = C_\pm (z/\ell)^{\lambda_\pm}, \tag{1}$$

where A is the projected area, and ℓ is the minimal lateral dimension. The subscripts $\pm$ are intended to distinguish the fitting parameters for plunging, C_+, λ_+, from those for withdrawing, C_-, λ_-. Generally, the exponents for plunging were $\lambda_+ \approx 1.3$, and for withdrawing the exponents consistently were $\lambda_- \approx 1.8$. For comparison, a linear dependence of the drag on the immersion depth is included in fig. 1b, which makes it clear that over several decades, the drag dependence truly is supra-linear. The best fits are reported in table II. Submerging the glass beads in water to reduce the gravitational force from $\rho g \approx 24\,\mathrm{kPa}$ to $\rho g \approx 14\,\mathrm{kPa}$, does

TABLE II – *Table summarizing power law behavior of plunging and withdrawing intruders of different shapes under different conditions.* * *The gravitational force, ρg has been modified to take into account the buoyancy of water.* ** *For plunging into freshly poured sand.*

	Plunging		Withdrawing	
Intruder shape	C_+	λ_+	C_-	λ_-
Glass beads in wide dish				
cube	21 ± 5	1.2 ± 0.3	-1.1 ± 0.6	1.9 ± 0.5
sphere	15 ± 3	1.2 ± 0.1	-1.2 ± 0.6	1.8 ± 0.3
vertical rod	10 ± 2	1.4 ± 0.1	-0.5 ± 0.2	1.7 ± 0.1
horizontal rod	9 ± 2	1.3 ± 0.1	-0.7 ± 0.1	1.6 ± 0.1
Glass beads in water*				
sphere	15 ± 4	1.5 ± 0.1	-1 ± 0.5	2 ± 0.2
Glass beads in narrow dish				
sphere	16 ± 6	1.3 ± 0.2	-2 ± 1	1.8 ± 0.3
Sand in wide dish				
horizontal rod	29 ± 7*	1 ± 0.2**	-0.6 ± 0.2	1.4 ± 0.4

not change the dynamics, which is similar to findings that complete immersion in water does not change the angle of repose [19].

The scaling of drag forces for horizontal rods of different aspect ratios, with diameter ℓ and length L was measured, and fig. 2 shows good collapse using this rescaling for plunging and withdrawing horizontal rods. The power law curve fits are consistent with those for intruders that only had one lateral length scale (*i.e.* spheres and cubes).

In order to investigate the effects of particle shape and roughness of the granular media, experiments for horizontal rods of different sizes were carried out using sifted sand ("play

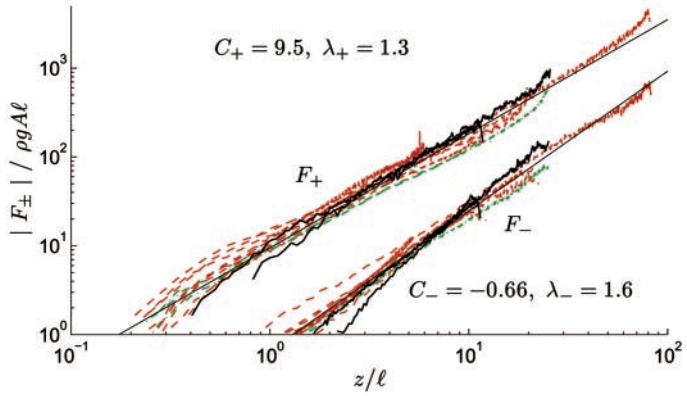

Fig. 2 – Rescaled plots of the plunging forces, F_+, and the withdrawal forces, F_- for horizontal rods in beds of monodisperse glass beads. Combinations of different dimensions, $\ell \times L$, and bead dimensions, d, are listed in table I. Best power-curve fits are overlaid, and the fitting constants for eq. (1) are shown.

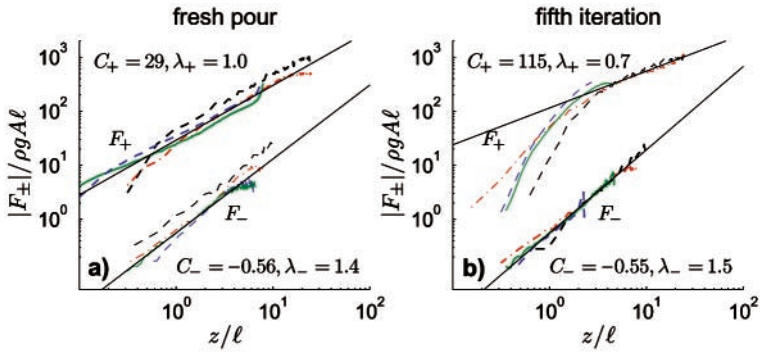

Fig. 3 – Rescaled plots of the drag forces of horizontal rods moving in a bed of sand: a) freshly poured and b) after four plunging/withdrawing iterations. Best fits are included, and for the fifth plunge the fit is for the region $z/\ell \geq 4$.

sand" purchased from Ace Hardware). While the withdrawing behavior for sand is close to that for glass beads (see table II), there were two notable differences in the plunging behavior of the sand: 1) the forces are considerably larger than for glass beads, 2) there is a history dependence, *i.e.* the results varied with successive trials. The history dependence can be seen by comparing the drag for *freshly* poured sand shown in fig. 3a with the plunging forces after *four* plunging/withdrawing iterations shown in fig. 3b. In both cases the rescaled forces collapse reasonably well. For the first trial the plunging force increases linearly with the immersion depth, while after successive plunges/withdrawals the plunging force is larger and cannot be fitted by a simple power-curve. Evidently, the shearing process introduces some change in the arrangement and orientation of the sand grains that leads to changes in the plunging force. As with glass beads, wrapping the horizontal rod in sandpaper affected the drag negligibly.

Discussion. – The results summarized in table II show a surprising degree of consistency in the prefactor and exponents of the power law (1) over a wide range of parameters. Taking into account the error bars, *all* withdrawal experiments show similar power law behavior: the exponents are clustered about $\lambda_- \approx 1.8$, and the prefactors are clustered about $C_- \approx -1$. Except for plunging in sand, *all* plunging experiments have similar power laws: $C_+ \approx 15$ and $\lambda_+ \approx 1.3$. In a related publication, the group of Schiffer [17], investigated how nearby boundaries increase the drag force on plunging intruders. They report that the drag force away from the bottom boundary increases in a nearly linear fashion; however, closer inspection of their data plots shows that sufficiently far away from the bottom boundary, the drag force has positive curvature, indicative of supra-linear immersion dependence. This trend is made apparent by the data reported here, since it spans over two decades in immersion depth, and a large range of bead diameters and intruder dimensions.

For static granular packs there are several models describing the stress fields, such as the Mohr-Coulomb failure analysis [2], Janssen's model for stresses in silos [20] and the "oriented stress linearity" model [3]. These models can account for interesting interactions of the stress fields with the container walls, and in practice the side walls are gently tapped in order to fully mobilize the wall friction [18]. In contrast, here the intruder's continuous motion keeps the granular medium locally fluidized, the container walls are far away, and there is no tapping.

A starting point for modeling the average force on the intruder is to consider the average contact stresses acting on the intruder's surface, which has components normal to the surface,

σ_{nn}, and along the surface, σ_{nt}, where $\hat{\boldsymbol{t}}$ is directed along the direction of the granular flow. Since the intruder is continually moving, the stresses on the granular media close to the intruder's surface are at failure. The tangential stresses due to shearing against the intruder surface are proportional to the normal stresses, as described by Coulomb's friction law, $\sigma_{nt} \approx \mu\sigma_{nn}$, where μ is of order 1. The average drag force is the surface integral $\boldsymbol{F} \approx \int_S (\sigma_{nn}\hat{\boldsymbol{n}} + \mu\sigma_{nn}\hat{\boldsymbol{t}})\mathrm{d}S$, where the first term is the pressure drop as in bluff body drag, and the second term is frictional drag. Dividing the measured drag forces by the intruder's projected area gives estimates for the average pressure for glass beads on the advancing surface:

$$\sigma_{nn} \approx \begin{cases} \mathcal{O}(10)\rho g z^{1.3}\ell^{-0.3} & \text{plunging,} \\ \mathcal{O}(1)\rho g z & \text{horizontal motion [10],} \\ \mathcal{O}(1)\rho g z^{1.8}\ell^{-0.8} & \text{withdrawing.} \end{cases} \tag{2}$$

In contrast to horizontal motion, where the granular drag pressure increases linearly with immersion depth, for vertical motion the drag increases more rapidly than the ambient granular pressure head $p = \rho g z$. It is interesting to contrast and compare this result with Stokes' drag on slender bodies (such as rods), where unlike granular media, the fore-aft pressure drop increases with velocity, v, and is independent of immersion depth. However similar to granular media, the pressure drop scales inversely with the narrowest dimension which sets the length scale for the flow around the rod: $\sigma_{nn} \sim \Delta p \propto v\ell^{-1}$ [21].

The disparity in the magnitude of the plunging and withdrawing normal stresses is not surprising, because the nature of the two types of granular flows is different. During plunging, particles in the path of the intruder are "squeezed out" sideways, occasionally experiencing strong dynamic force chains, whereas particles in the path of a withdrawing intruder can simply move up collectively with particles continually falling out of the shrinking region of upward-moving particles. The similarity in the withdrawing results for sand and glass beads indicate a more universal behavior that is independent of the history and particle shape, whereas the difference in the plunging forces for sand and glass beads shows that plunging is strongly influenced by the shape of the particles.

While in the experiments reported here the plunging forces are always larger than the withdrawal forces, extrapolation of eq. (2) indicates that there may be a crossing point, $z \approx 10^3\ell$, where the plunging forces may be *less* than the withdrawing forces. Further experiments in larger granular beds (about 1 meter in size) are necessary to verify this prediction.

Conclusions. – There are very few continuum models for dynamic dense granular systems. An elementary model by Albert *et al.* [22] for drag in glass beads treats the force chains as springs whose spring constants, $k \sim \rho g z d$, increase linearly with depth and break when a critical compressive force has been achieved, $F_{\mathrm{crit}} \sim kz$. This leads to normal stresses, σ_{nn}, that increase linearly with immersion depth, which agrees with certain drag experiments in the *horizontal* direction using glass beads, and disagrees with other drag experiments where sand is used as a granular medium [9]. But the data reported here clearly shows a non-linear dependence of the drag on the immersion depth. For glass beads and the three directions investigated so far, horizontal, withdrawing and plunging, three different types of drag behavior have been found, and quite likely for motion in other directions other different types of drag behavior will be found.

The drag forces on slowly plunging and withdrawing intruders in dense beds of monodisperse glass beads and monodisperse, freshly poured sand show simple power law behavior that only depends on the intruder's lateral dimensions and immersion depth. Unlike sand, there is little history dependence on shearing for glass beads. The power laws should prove

helpful for theorists formulating the granular equivalent of Stokes drag in fluids, and generally serve as a model system for developing continuum, mean-field theory of non-conservative, non-equilibrium, non-inertial driven systems. In contrast to the results here, very recent experimental and theoretical work for ballistic intruders ($v > 1$ m/s) falling into granular beds (*e.g.* meteor strikes), show that the drag force has little immersion dependence and instead depends strongly on the impact velocity [23, 24].

* * *

The author thanks P. Mucha and E. R. Weeks for helpful discussions.

REFERENCES

[1] de Gennes P. G., *Rev. Mod. Phys.*, **71** (1999) S374.
[2] Nedderman R. M., *Statistics and Kinematics of Granular Materials* (Cambridge University Press, Cambridge, UK) 1992.
[3] Vanel L., Claudin P., Bouchaud J. P., Cates M. E., Clement E. and Wittmer J.P., *Phys. Rev. Lett.*, **84** (2000) 1439.
[4] Duran J., *Sands, Powders and Grains* (Springer, New York) 2000.
[5] Bocquet L., Losert W., Schalk D., Lubensky T. C. and Gollub J. P., *Phys. Rev. E*, **65** (2002) 0113071.
[6] Makse H. A. and Kurchan J., *Nature*, **415** (2002) 614.
[7] Jenkins J. T. and Zhang C., *Phys. Fluids*, **14** (2002) 1228.
[8] Volfson D., Tsimring L. S. and Aranson I. S., *Phys. Rev. E*, **68** (2003) 0213011.
[9] Wieghardt K., *Mech. Res. Commun.*, **1** (1974) 3.
[10] Albert R., Pfeifer M. A., Barabasi A. L. and Schiffer P., *Phys. Rev. Lett.*, **82** (1999) 205.
[11] Wassgren C. R., Cordova J. A., Zenit R. and Karion A., *Phys. Fluids*, **15** (2003) 3318.
[12] Chehata D., Zenit R. and Wassgren C. R., *Phys. Fluids*, **15** (2003) 1622.
[13] Atkinson T. D., Butcher J. C., Izard M. J. and Nedderman R. M., *Chem. Eng. Sci.*, **38** (1983) 91.
[14] Albert I., Tegzes P., Albert R., Sample J. G., Barabasi A. L., Vicsek T., Kahng B. and Schiffer P., *Phys. Rev. E*, **64** (2001) 031307.
[15] Arroyo-Cetto D., Pulos G., Zenit R., Jimenez-Zapata M. A. and Wassgren C. R., *Phys. Rev. E*, **68** (2003) 051301.
[16] Zhou F., Advani S. G. and Wetzel E. D., *Phys. Rev. E*, **69** (2004) 061306.
[17] Stone M. B., Bernstein D. P., Barry R., Pelc M. D., Tsui Y. K. and Schiffer P., *Nature*, **247** (2004) 503.
[18] Horvath V. K., Janosi I. M. and Vella P. J., *Phys. Rev. E*, **54** (1996) 2005.
[19] Samadani A. and Kudrolli A., *Phys. Rev. E*, **64** (2001) 051301.
[20] Janssen H. A., *Z. Vereins Deutsch Ing.*, **39** (1895) 1045.
[21] Batchelor G. K., *J. Fluid Mech.*, **44** (1970) 419 .
[22] Albert I., Tegzes P., Kahng B., Sample J. G., Pfeifer A. L., Vicsek T. and Schiffer P., *Phys. Rev. Lett.*, **84** (2000) 5122.
[23] Ciamarra M. P., Lara A. H., Lee A. T., Goldman D. I., Vishik I. and Swinney H. L., *Phys. Rev. Lett.*, **92** (2004) 194301.
[24] Uehara J. S., Ambroso M. A., Ojha R. P. and D. J. Durian, *Phys. Rev. Lett.*, **90** (2003) 194301.